



ELSEVIER

Available online at www.sciencedirect.com

SCIENCE @ DIRECT®

PHYSICS LETTERS B

Physics Letters B 621 (2005) 81–88

www.elsevier.com/locate/physletb

Decoupling of valence neutrons from the core in ^{17}B

Zs. Dombrádi^a, Z. Elekes^{a,b}, R. Kanungo^{b,1}, H. Baba^c, Zs. Fülöp^a, J. Gibelin^d,
Á. Horváth^e, E. Ideguchi^f, Y. Ichikawa^f, N. Iwasa^g, H. Iwasaki^f, S. Kanno^c,
S. Kawai^c, Y. Kondo^h, T. Motobayashi^b, M. Notani^f, T. Ohnishi^f, A. Ozawaⁱ,
H. Sakurai^f, S. Shimoura^f, E. Takeshita^c, S. Takeuchi^b, I. Tanihata^j, Y. Togano^c,
C. Wu^b, Y. Yamaguchi^c, Y. Yanagisawa^b, A. Yoshida^b, K. Yoshida^b

^a *Institute of Nuclear Research of the Hungarian Academy of Sciences, PO Box 51, H-4001 Debrecen, Hungary*

^b *The Institute of Physical and Chemical Research (RIKEN), 2-1 Hirosawa, Wako, Saitama 351-0198, Japan*

^c *Rikkyo University, 3 Nishi-Ikebukuro, Toshima, Tokyo 171, Japan*

^d *Institut de Physique Nucléaire, 15 rue Georges Clemenceau, F-91406 Orsay, France*

^e *Eötvös Loránd University, Pázmány Peter sétány 1/A, H-1117 Budapest, Hungary*

^f *University of Tokyo, Tokyo 1130033, Japan*

^g *Tohoku University, Sendai, Miyagi 9808578, Japan*

^h *Tokyo Institute of Technology, 2-12-1 Oh-Okayama, Meguro, Tokyo 152-8551, Japan*

ⁱ *University of Tsukuba, Ibaraki 305-8571, Japan*

^j *Argonne National Laboratory, 9700 S. Cass Avenue, Argonne, IL 60439, USA*

Received 8 March 2005; received in revised form 13 June 2005; accepted 13 June 2005

Available online 21 June 2005

Editor: D.F. Geesaman

Abstract

Proton inelastic scattering study of ^{17}B nucleus has been performed at 43.8 A MeV average energy in inverse kinematics using a liquid hydrogen target. In the Doppler corrected γ ray spectrum, a single peak with an energy of 1089(15) keV appeared corresponding to the first excited state of ^{17}B . Based on the reaction cross section, $\beta_2^{pp'}$ deformation parameter of the transition is deduced by distorted wave analysis. Comparing it with the electric quadrupole moment of the nucleus, it is shown that the deformation of the neutron distribution is large ($\beta_n \sim 0.6$), and the neutron effective charge is much smaller ($e_n < 0.12$) than usual (~ 0.5). The small effective charge is interpreted as a consequence of the decoupling of valence neutrons from the core.
© 2005 Elsevier B.V. All rights reserved.

PACS: 23.20.Lv; 25.40.Ep; 29.30.Kv; 27.30.+t

E-mail address: elekes@atomki.hu (Z. Elekes).

¹ Present address: TRIUMF, 4004 Wesbrook Mall, Vancouver, BC V6T 2A3, Canada.

0370-2693/\$ – see front matter © 2005 Elsevier B.V. All rights reserved.

doi:10.1016/j.physletb.2005.06.031

Nuclei close to the neutron dripline having loosely bound valence neutrons have been studied intensively because their properties deviate from those of the stable nuclei. One of the most exotic structures in nuclei near the dripline is the neutron halo discovered about 20 years ago via the determination of the matter radii of nuclei [1]. Since then, it has been shown that—although the well-developed neutron halo is a relatively rare phenomenon—an extended but more limited nucleon distribution is quite common for nuclei with large N/Z ratios. This large ratio results in a large difference in the Fermi energies of protons and neutrons and, consequently, leads to the weakening of the strong correlation of proton and neutron distributions characteristic for stable nuclei [2]. In this way, the halo or skin neutrons can be decoupled from the nuclear core, and move independently of the rest of the nucleus. An example for their independent relative motion is the pygmy dipole resonance where—exploiting the suppressed interaction between the valence nucleons in the halo and the core nucleons—the weakly bound neutrons are forced to move independently of the core via an electric dipole interaction. Such phenomenon was observed in several nuclei close to the neutron dripline [3–5]. As a new decoupling feature, the decrease of the neutron effective charge was proposed [6]. The loosely bound particles spend an appreciable amount of time outside of the core, therefore, due to the short range of the nuclear interaction, they cannot interact with it, and thus, cannot polarize the core. As a consequence, the quadrupole polarization charges in nuclei with an extended neutron distribution are expected to be strongly reduced [7].

Experimentally, the decrease of the neutron polarization charge can be observed by a comparison of the intensities of the electric quadrupole processes where either the proton or the neutron quadrupole properties are dominant. The ratio of the neutron and proton multipole transition matrix elements, M_n/M_p , depends only on the core polarization parameters in single closed shell nuclei [8]. Any change in the M_n/M_p ratio along such an isotopic chain would be a consequence of the changes in the polarization process, which leads also to the change of the effective charges. Recent results show that the M_n/M_p ratio in ^{20}O is significantly larger than the corresponding value in ^{18}O [8]. This suggests that the strength of the core polarization is decreased in ^{20}O [9].

Very recently, an extremely large $M_n/M_p \sim 4N/Z$ ratio was observed in ^{16}C by use of the Coulomb-nuclear interference method [10], and confirmed by the comparison of the $B(E2)$ value [11] with the result of (p, p') scattering study [12]. In this nucleus, the neutron effective charge of $e_n = 0.15$ was deduced [10]. This value is much smaller than usual in this region ($e_n = 0.5$), and can be considered as a clear indication of the decoupling of the valence neutrons from the ^{14}C core.

^{17}B is another nucleus where a significant decoupling may take place. The electric quadrupole moment of its ground state was measured at $Q = 38.6 \pm 1.5$ mb [13], which is very close to that of the $N = 8$ isotope ^{13}B , in contrast with the results of the shell model calculations, which—assuming the conventional $e_n = 0.5$ value for neutron effective charge—predict an increasing quadrupole moment with increasing mass. It was proposed that the deviation from the shell model is caused by the decrease of the neutron effective charge, which can lead to a constant or even slightly decreasing mass dependence of the quadrupole moment. The decreased effective charge may be a consequence of the decoupling of the valence neutrons from the core [13], but other sources of the deviation can also be conceivable. To check whether the shell model describes the quadrupole properties of the neutron distribution—considering that neutron skin or halo properties observed in this nucleus [14] are not included in that model—and to exclude other explanations like a decrease of the proton effective charge, which is also predicted for nuclei far from the stability [15], experimental information on the quadrupole moment of the neutron distribution is needed for ^{17}B . Unfortunately, it cannot be measured directly, only the transitional moment can be determined, e.g., via inelastic scattering. To deduce the neutron deformation, we studied the inelastic scattering of ^{17}B in inverse kinematics.

In the present experiment, we employed the technique of in-beam γ -ray spectroscopy incorporating inelastic proton scattering [16] and utilizing a liquid hydrogen target for enhancement of luminosity [17]. The experiment was done at the RIPS [18] beamline of the RIKEN accelerator research facility (see Fig. 1 for experimental setup). A ^9Be production target of 0.8 cm thickness was bombarded by a ^{22}Ne primary beam of 100 pA intensity and 110 A MeV energy. A secondary cocktail beam containing ^{17}B at

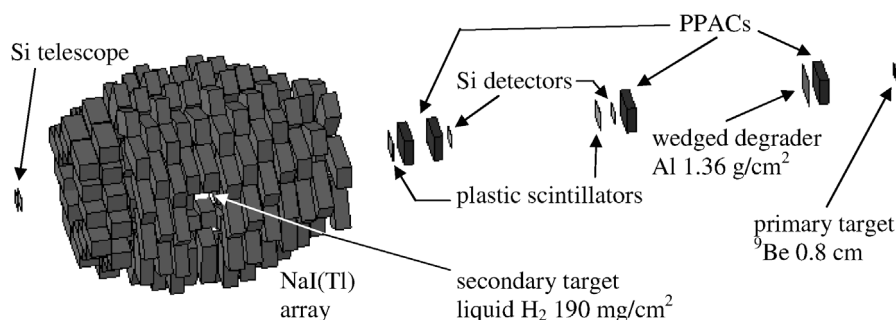


Fig. 1. Schematic view of the experimental setup. The figure is not to scale.

25% was produced after momentum and mass analysis by using a 1.36 g/cm^2 thick aluminum wedged degrader at the momentum dispersive focal plane (F1). In order to have a high beam intensity, the momentum acceptance of the fragment separator was set to a maximum value of 6%. In this way, around 200 pps rate could be achieved for ^{17}B . On an event by event basis, an identification of the incoming beam was performed by energy-loss, time-of-flight (TOF) and magnetic rigidity ($B\rho$) measurements. The $B\rho$ was determined using a parallel plate avalanche counter (PPAC) with an area of $15 \times 10 \text{ cm}^2$ at F1 covering the total momentum range of the secondary beam. The TOF was measured by plastic scintillators of 0.5 mm thicknesses placed at the first and second focal planes (F2 and F3) while two silicon detectors of 0.35 mm thickness were put at F2 and F3 providing the energy-loss information. With this method, the ^{17}B particles could be fully separated from other beam species.

The secondary beam hit a liquid hydrogen target placed at F3 which was 3 cm in diameter and 24 mm in thickness having an average areal density of 190 mg/cm^2 (the uncertainty of the areal density is around 10%) and it was closed by $6.6 \mu\text{m}$ thick Aramid foils [19]. The mean energy of the ^{17}B isotopes was calculated to be 43.8 A MeV taking into account the incident energy and the energy-loss information. The incident beam focusing was monitored by two PPACs placed at F3. The horizontal spot size of the beam was 20 mm while the vertical one was 18 mm in FWHM. In order to reduce the background events produced by the beam particles hitting the target holder were filtered out by putting a gate on the projected image of the beam on the target.

A silicon telescope with layers of 0.5, 2, 2 and 0.5 mm thicknesses was inserted in air at about 80 cm downstream of the target to identify the scattered particles. (The accelerator tube was closed by a thin Al plate of 1.5 mm.) The active area of the silicon detectors was $48 \times 48 \text{ mm}^2$ covering scattering angles between $0\text{--}1.7^\circ$. The inelastically scattered ^{17}B particles were stopped in the second and third layers and could be easily separated by the $\Delta E\text{--}E$ method from other boron nuclei emerging from the liquid hydrogen target by neutron removal reactions. The separation was done by requiring γ rays to be in coincidence with the telescope events, and linearizing the gated $\Delta E\text{--}E$ curves with second degree polynomials [20].

For the detection of the de-exciting γ rays, the DALI2 setup consisting of 158 NaI(Tl) scintillators [21] was put around the liquid hydrogen target. The prompt events were selected by putting a narrow time gate on the calibrated time spectrum of the NaI(Tl) detectors (see top panel of Fig. 2 for the resulting Doppler corrected spectrum of γ rays for ^{17}B). A low energy continuous background radiation was emitted from the thick Al/Si stack at the downstream direction. It could be eliminated by subtracting background contributions (e.g., target holder windows) estimated from the data taken without the liquid hydrogen but leaving the target holder unchanged (see middle panel of Fig. 2 for background contributions). The bottom panel of Fig. 2 shows the subtracted Doppler corrected spectra of γ rays for ^{17}B . A single peak at 1089(15) keV can be seen in the figure, which corresponds to the transition between the first excited and the ground state. This energy value is in agreement with the 1070(10) keV of Kondo et al. reported earlier [22] and confirmed by Kanungo et al. [23].

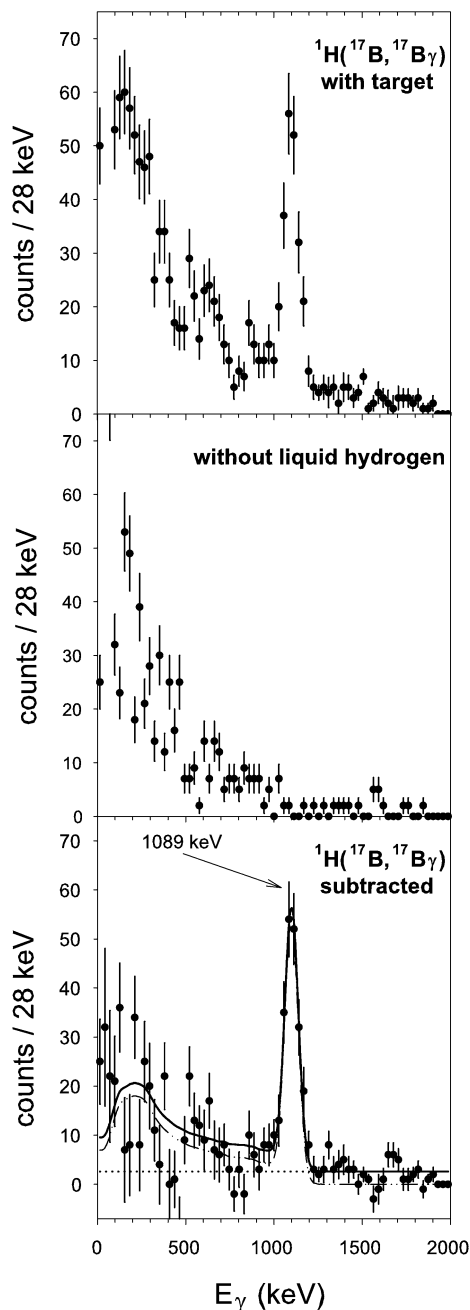


Fig. 2. Doppler-corrected spectra of γ rays emerging from $^1\text{H}(^{17}\text{B}, ^{17}\text{B}\gamma)$ reaction can be seen at the top of the figure. The middle spectrum is taken without the liquid hydrogen, while the spectrum in the bottom panel is produced by subtracting the two spectra. The solid line is the final fit including the spectrum curves from GEANT4 simulation (dashed line) and an additional constant background plotted as separate dotted line.

The peak position and its uncertainty was determined by fitting the spectra with a Gaussian function and constant backgrounds. The width of the peak was set to the expected value including the intrinsic resolution and Doppler effect. In order to retrieve the detector photo-peak efficiency, the peak position was fed into the detector simulation software GEANT4 [24] and the resultant response curves plus a small constant background are plotted in Fig. 2.

The integrated experimental cross section for the excitation of the first excited state in ^{17}B was determined to be $\sigma(0-1.7^\circ) = 9.4 \pm 1.2$ mb. To derive the quadrupole deformation parameter ($\beta_2^{pp'}$), a distorted wave calculation was performed using the ECIS79 [25] code. The standard collective form factors were applied in the analysis together with the optical potential parameters determined from the global phenomenological set CH89 [26]. The efficiency of the telescope was simulated by GEANT4 software [24] by using the experimental beam spot size as an input parameter. The simulated angular dependence of the efficiency was folded with the angular distribution of the ECIS curve when calculating the deformation parameters.

Fig. 3 shows the angular distribution of the γ rays emerging from $^1\text{H}(^{17}\text{B}, ^{17}\text{B}\gamma)$ reaction with respect to the beam direction. The experimental data can be fitted with an assumption of a $\Delta\ell = 1$ stretched dipole transition represented by a solid line in the figure and contradict to a supposed $\Delta\ell = 2$ quadrupole nature of the transition using realistic parameters during the fitting procedure. Therefore, a $3/2^-$ ground state followed by an $5/2^-$ excited state predicted by all available shell model [27,28] and AMD calculations [29] is a natural assumption. In this way, we got $\beta_2^{pp'} = 0.57 \pm 0.05$ value and deformation length of $\delta^{pp'} = \beta_2^{pp'} R = 1.76 \pm 0.15$ fm. There can be an additional systematic error coming from the uncertainty in choice of the optical potential parameters. It was shown for ^6He that CH89 can reproduce the elastic scattering data on protons only with a modification by an additional polarization potential [30]. At the same time, CH89 was appropriate for fitting the inelastic channel of proton scattering on $^{18,20}\text{O}$ nuclei [9]. Furthermore, in a recent study, CH89 also showed a good agreement with the angular distribution of the inelastic scattering data in the $p + ^{16}\text{C}$ reaction [12]. In

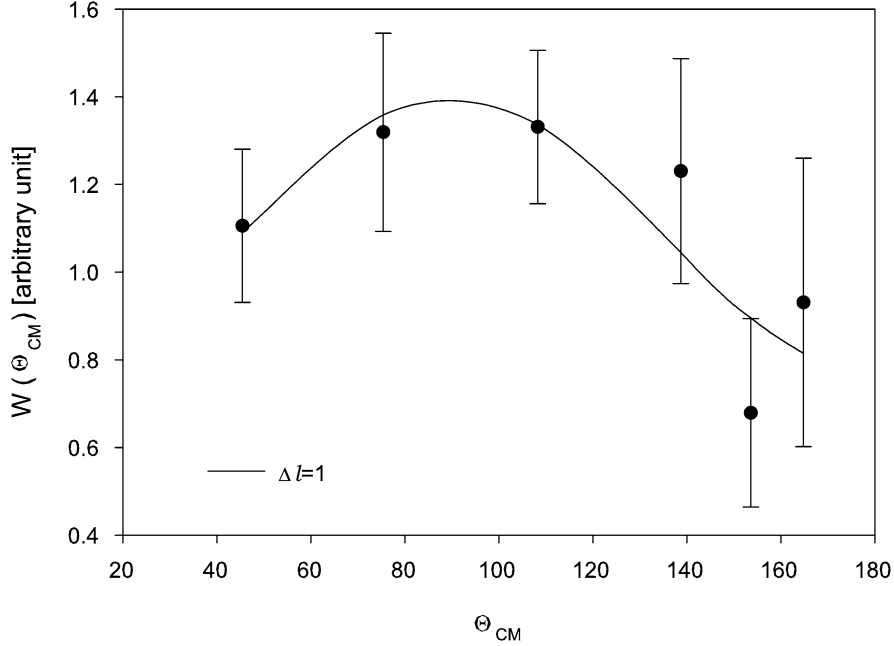


Fig. 3. Angular distribution of γ rays emerging from $^1\text{H}(^{17}\text{B}, ^{17}\text{B})$ reaction with respect to the beam direction. The solid line represents a fit with an assumption of a dipole $L = 1$ transition.

any case, the systematic error was checked first with a phenomenological optical model parameters deduced recently using scattering data on nuclei with $A > 23$ [31] and found 3% difference for the deformation parameter. Secondly, the real part of the CH89 optical model parameter set was reduced suggested in Ref. [30] by 20% as an extreme change and 15% difference was observed in the deformation parameter. This kind of systematic error leads to a $\delta\beta = 0.1$ uncertainty.

If we allow different deformations for the protons and neutrons, the quadrupole deformation parameter deduced is not the deformation of the nucleus anymore. It is an average of the proton and neutron deformations, which depends on the type of the probe used. The (p, p') reaction is 3 times more sensitive to the neutron than to the proton deformation, thus, the deformation value obtained comes mainly from the deformation of the neutron distribution. To calculate the proton and neutron deformations, the above information should be combined with the result of a probe sensitive mainly to the deformation of the proton distribution like the already measured electric quadrupole moment [13].

The electric quadrupole moment can be written as a sum of the proton and neutron contributions

$$Q = e_n Q_n + e_p Q_p, \quad (1)$$

where e_p and e_n are the proton and neutron effective charges, while Q_p and Q_n are the proton and neutron quadrupole moments. This is the spectroscopic quadrupole moment, which can be measured experimentally in the laboratory frame. On the other hand, in the case of a deformed nucleus it is instructive to convert the quadrupole moment to the intrinsic frame of reference determined by the deformation axis of the nucleus, since the intrinsic quadrupole moment (Q_0) can be connected to the geometric properties of the nucleus.

For example, Q_0 , and consequently Q , can be expressed in terms of the rotational model using proton and neutron deformation parameters (β_p, β_n). Considering a $J = 3/2$ spin for the ground state of ^{17}B , the quadrupole moment can be expressed as

$$\begin{aligned} Q &= Q_0 \frac{3K^2 - J(J+1)}{(J+1)(2J+3)} \\ &= \frac{3}{5\sqrt{5}\pi} R^2 (e_n N \beta_n + e_p Z \beta_p), \end{aligned} \quad (2)$$

where R , N and Z are the nuclear radius, the neutron and the proton numbers, respectively. The ratio Q_n/Q_p in the rotational model is just the same as the ratio of the transition matrix elements M_n/M_p which in turn can be connected to the characteristic quantities of the (p, p') probe by the Bernstein formula [32]. In this way, we get

$$\frac{Q_n}{Q_p} = \frac{N\beta_n}{Z\beta_p} = \frac{M_n}{M_p} = \frac{b_p}{b_n} \left[\frac{\delta^{pp'}}{\beta_p R} \left(1 + \frac{b_n N}{b_p Z} \right) - 1 \right], \quad (3)$$

where $b_n/b_p = 3$ are the sensitivity parameters for protons and neutrons of our (p, p') probe. Combining Eqs. (2) and (3) the unknown deformation parameter β_n can be expressed by the measured quantities Q and $\delta^{pp'}$ as a function of the effective charges e_n, e_p :

$$\beta_n = \frac{\frac{b_p}{b_n N} \left[\frac{e_p Z \delta^{pp'}}{R} \left(1 + \frac{b_n N}{b_p Z} \right) - \frac{5\sqrt{5\pi} Q}{3R^2} \right]}{\left(e_p - e_n \frac{b_p}{b_n} \right)} = \frac{C e_p - D}{e_p - \frac{1}{3} e_n}, \quad (4)$$

$$\beta_p = \frac{\frac{5\sqrt{5\pi} Q}{3R^2} - \frac{e_n Z b_p \delta^{pp'}}{b_n R} \left(1 + \frac{b_n N}{b_p Z} \right)}{\left(e_p - e_n \frac{b_p}{b_n} \right) Z} = \frac{A - B e_n}{e_p - \frac{1}{3} e_n}. \quad (5)$$

For a qualitative analysis of the relations between the deformation parameters and the effective charges, we can consider that e_n is small compared to e_p , i.e., $\frac{1}{3}e_n$ can be neglected in the denominators. Actually, this approximation is in accordance with the usual assumption of $e_n = 0$ used in comparison of the transitional matrix elements M_n, M_p . In this way,

$$\beta_n \approx C - \frac{D}{e_p} = 0.65 - \frac{0.07}{e_p} \approx 0.6, \quad (6)$$

$$\beta_p e_p \approx A - B e_n = 0.54 - 1.56 e_n. \quad (7)$$

Eq. (6) shows that the deformation parameter β_n only slightly depends on the effective charges and its value of 0.6 is relatively large, which is close to the neutron deformation observed in ^{16}C . Having β_n (consequently δ_n), the value of β_p (consequently δ_p) can also be deduced by the formula

$$(N b_n + Z b_p) \delta^{pp'} = N b_n \delta_n + Z b_p \delta_p. \quad (8)$$

From $\beta_n \approx 0.6$ and $\delta^{pp'} = 1.76 \pm 0.15$ fm, $\beta_p \approx 0.36$ and $M_n/M_p \approx 4.0$ can be derived.

The proton and neutron deformations can be deduced to be $\beta_n \sim \beta_p \sim 0.35$ from the quadrupole moments calculated in the frame of the shell model. Comparing this data with our results, the calculated proton deformation is in agreement with our value deduced from the comparison of $\delta^{pp'}$ and Q , while our neutron deformation is more than 50% larger than the calculated one. Having such huge a deformation, a strongly reduced neutron effective charge is needed to explain the low value of the electric quadrupole moment independently of the value of the proton effective charge.

Using Eq. (7) and assuming the lowest possible $e_p = 1$ value for proton effective charge, an upper limit of $e_n < 0.12$ can be given for the neutron effective charge, which is 4 times smaller than the usual value characteristic for the valley of stability. This experimental upper limit fits well the results obtained from comparison of model calculations with probes sensitive to different aspects of nuclear matter distributions. Ogawa et al. proposed $e_n \approx 0.1$ [13] from a comparison of the shell model calculations and their quadrupole moment measurement, while Kondo et al. deduced $e_n \approx 0$ setting their deformation length determined by inelastic scattering on ^{12}C against the one calculated from shell model [33]. It is worth mentioning that both probes are very sensitive to the value of the proton effective charge, and in the case of $e_p = 1$ both probes give an upper limit of $e_n \sim 0.3$ for the neutron effective charge.

Recently, Sagawa et al. [15] has given a simple parametrization on the isospin dependence of the polarization charges deduced from mean field + random phase approximation calculations

$$e_{\text{pol}} = 0.82 \frac{Z}{A} - 0.25 \frac{N - Z}{A} + \left(0.12 - 0.36 \frac{Z}{A} \frac{N - Z}{A} \right) \tau_z, \quad (9)$$

where τ_z is 1 for neutrons and -1 for protons. Using this approximation, the neutron polarization charge (consequently e_n) is 0.21 for ^{17}B . This effect may explain half of the decrease of the neutron effective charge observed in the present work.

It is interesting to note that in both ^{16}C and ^{17}B the small neutron effective charge is accompanied with a large neutron deformation, a feature not observed in other neutron rich nuclei studied by the same method like ^{28}Ne or ^{34}Mg [34]. The two properties may have

a common root. Both ^{16}C and ^{17}B have neutron skin [14]. Applying the empirical relation introduced by Hansen and Jonson [35], one can estimate the valence neutron radius in ^{16}C and ^{17}B , too, assuming a core + 2-neutron (for ^{16}C) and a core + 4-neutron (for ^{17}B) structure. Knowing the mass radius (r_m) and the radius of the core (r_c), the radius of the valence neutron distribution (r_v) can be estimated as

$$r_m^2 = (A - 2)/A[r_c^2 + (2/A)r_v^2]. \quad (10)$$

From reaction cross section measurements the radii of the nuclei of interest as well as the radii of their cores were determined [14]. Consequently, the radius of the valence neutron distribution can be estimated to be $r_v = 4.9 \pm 0.4$ fm. Since the neutron radius is ~ 1.2 fm, the ground state of the ^{16}C nucleus can be modeled as a larger sphere of the ^{14}C core with a radius of 2.3 fm [14] touching the smaller spheres of the two valence neutrons of 1.2 fm radius each. Because the neutrons are on time mirrored orbits, they are expected to be on the opposite sides of the core [36]. Such an arrangement leads to a shape with about 2 : 1 axis ratio, which is in a qualitative agreement with the experimental value of neutron deformation of ^{16}C determined to be $\beta_n \approx 0.7$ [10]. Although it is less trivial to give an estimate on the spatial distribution of the four neutrons, an arrangement with a closed $N = 8$ neutron shell + 2 pairs of neutrons outside of it sitting on the two lowest Ω Nilsson orbits is in agreement with the predictions of the AMD model [29]. The large valence neutron radius not only contributes to the increased neutron deformation, but may be responsible also for the decreased effective charge. The valence neutron radius is large enough to let the valence neutrons spend a substantial time out of the core reducing their interaction. Quantitative calculations show that the increased valence radius reduces the core polarization by about 50% [6]. For the other half of its decrease observed in the present work, the isospin dependence of the particle-vibration coupling strength is expected to be responsible.

Summarizing our results, we have measured the excitation cross section of the $^{17}\text{B}(p, p')$ reaction. From a comparison with the previously determined electric quadrupole moment, we deduced the deformation parameter of the neutron and proton distributions to be $\beta_n \sim 0.6$ and $\beta_p = 0.36$. Exploiting the information on deformations in the ground state of ^{17}B an up-

per limit on the neutron effective charge of $e_n < 0.12$ has been deduced. This value is 4 times smaller than the one characteristic for nuclei close to stability in this mass region. It is comparable with the value expected from the decoupling of valence neutrons from the nuclear core due to the large isospin and the large radius of the valence neutron orbits. The increased valence neutron radius may be responsible also for the large neutron deformation observed in both ^{16}C and ^{17}B . The decoupling phenomenon was shown previously in ^{16}C , now we proved its existences in ^{17}B , too, and there are suggestions—from a comparison with shell model calculations—that it takes place also in ^{15}B [33].

Acknowledgements

We would like to thank the RIKEN Ring Cyclotron staff for their assist during the experiment. One of authors (Z.E.) is grateful for the JSPS Fellowship Program in RIKEN and the Bolyai grant in Hungary. The European authors thank the kind hospitality and support from RIKEN. The present work was partly supported by the Grant-in-Aid for Scientific Research (No. 1520417) by the Ministry of Education, Culture, Sports, Science and Technology and by OTKA T46901, T42733, T38404, T32113.

References

- [1] I. Tanihata, et al., Phys. Rev. Lett. 55 (1985) 2676.
- [2] A. Ozawa, et al., Nucl. Phys. A 693 (2001) 32.
- [3] D.J. Millener, et al., Phys. Rev. C 83 (1983) 497.
- [4] M. Zinser, et al., Nucl. Phys. A 619 (1997) 151.
- [5] T. Nakamura, et al., Phys. Rev. Lett. 83 (1999) 1112.
- [6] H. Sagawa, et al., Phys. Rev. C 63 (2001) 064310.
- [7] H. Sagawa, Eur. Phys. J. A 13 (2002) 87.
- [8] J.K. Jewell, et al., Phys. Lett. B 454 (1999) 181.
- [9] E. Khan, et al., Phys. Lett. B 490 (2000) 45.
- [10] Z. Elekes, et al., Phys. Lett. B 586 (2004) 34.
- [11] N. Imai, et al., Phys. Rev. Lett. 92 (2004) 062501.
- [12] H.J. Ong, et al., Phys. Rev. C, in press.
- [13] H. Ogawa, et al., Phys. Rev. C 67 (2003) 064308.
- [14] A. Ozawa, et al., Nucl. Phys. A 691 (2001) 599.
- [15] H. Sagawa, et al., Phys. Rev. C 70 (2004) 054316.
- [16] H. Iwasaki, et al., Phys. Lett. B 481 (2000) 7.
- [17] Y. Yanagisawa, et al., Phys. Lett. B 566 (2003) 84.
- [18] T. Kubo, et al., Nucl. Instrum. Methods B 70 (1992) 309.
- [19] H. Akiyoshi, et al., RIKEN Accel. Prog. Rep. B 32 (1998) 167.

- [20] Z. Elekes, et al., *Phys. Lett. B* 599 (2004) 17.
- [21] S. Takeuchi, et al., *RIKEN Accel. Prog. Rep.* 36 (2003) 148.
- [22] Y. Kondo, et al., *RIKEN Accel. Prog. Rep.* 36 (2003) 65.
- [23] R. Kanungo, et al., *Phys. Lett. B* 608 (2005) 206.
- [24] S. Agostinelli, et al., *Nucl. Instrum. Methods A* 506 (2003) 250.
- [25] J. Raynal, *Phys. Rev. C* 23 (1981) 2571.
- [26] R.L. Varner, et al., *Phys. Rep.* 201 (1991) 57.
- [27] E.K. Warburton, et al., *Phys. Rev. C* 46 (1992) 923.
- [28] N.A.F.M. Poppelier, et al., *Phys. Lett. B* 157 (1985) 120.
- [29] Y. Kanada-Enyo, et al., *Phys. Rev. C* 52 (1995) 647.
- [30] V. Lapoux, et al., *Phys. Lett. B* 517 (2001) 18.
- [31] A.J. Koning, et al., *Nucl. Phys. A* 713 (2003) 231.
- [32] A.M. Bernstein, et al., *Phys. Rev. Lett.* 42 (1979) 425.
- [33] Y. Kondo, et al., *Phys. Rev. C* 71 (2005) 044611.
- [34] Z. Elekes, et al., *ATOMKI Annual Report*, 2003, p. 15.
- [35] P.G. Hansen, et al., *Europhys. Lett.* 4 (1987) 409.
- [36] M.V. Zhukov, et al., *Phys. Scr.* 25 (1982) 522.